JACS
JOURNAL OF THE AMERICAN CHEMICAL SOCIETY
Communication
pubs.acs.org/JACS

Graphene Quantum Dots Supported by Graphene Nanoribbons with Ultrahigh Electrocatalytic Performance for Oxygen Reduction

Huile Jin,[†] Huihui Huang,[†] Yuhua He,[†] Xin Feng,[†] Shun Wang,*[,†] Liming Dai,*[,‡] and Jichang Wang*[,†,§]

[†]College of Chemistry and Materials Engineering, Wenzhou University, Wenzhou, Zhejiang 325035, China

[‡]Department of Macromolecular Science and Engineering, School of Engineering, Case Western Reserve University, Cleveland, Ohio 44106, United States

[§]Department of Chemistry and Biochemistry, University of Windsor, Windsor, Ontario N9B 3P4, Canada

Supporting Information

ABSTRACT: A new class of oxygen reduction reaction (ORR) catalysts based on graphene quantum dots (GQDs) supported by graphene nanoribbons (GNRs) has been developed through a one-step simultaneous reduction reaction, leading to ultrahigh performance for O reduction with an excellent electrocatalytic activity (higher limiting current density and lower overpotential than those of platinum) and high selectivity and stability in alkaline media comparable to the best C-based ORR catalysts reported so far. Electron microscopy revealed numerous surface/edge defects on the GQD/GNR surfaces and at their interface to act as the active sites. This, coupled with efficient charge transfer between the intimately contacted GQDs and GNRs, rationalized the observed ultrahigh electrocatalytic performance for the resultant GQD-GNR hybrids. Thus, this study opens a new direction for developing low-cost, highly efficient, C-based ORR electrocatalysts.

Oxygen reduction reaction (ORR) plays an important role in fuel cells and next-generation metal−air batteries.[1] Catalysts are required to promote the ORR at the cathode in fuel cells and metal−air batteries for energy conversion and storage. Pt-based precious metals have been known as the most efficient ORR catalyst.[2] However, the high cost and poor durability are two major drawbacks hindering the widespread application of Pt-based catalysts.[3] To overcome these problems, considerable attention has been paid to the development of nonprecious metal[4] and even metal-free ORR catalysts.[5] Promising results have been reported on transition metal N_4-macrocycles compounds,[6] transition metal sulfides,[7] oxides,[8] or carbides,[9] and heteroatom-doped C materials.[10] Among them, heteroatom-doped C is one of the promising cathode catalysts for ORR.

Recently, a wide range of heteroatom (e.g., N, B, S, P, or I) mono- and codoped C materials, including carbon nanotubes (CNTs),[11] graphene,[12] graphite,[13] and mesoporous C,[14] have been reported to exhibit ORR activities comparable to commercial Pt/C catalysts, without CO poisoning or methanol-crossover effect.[15] Of particular interest, Qu et al. have reported that N-doped graphene quantum dots (GQDs) with O-rich functional groups exhibited superb electrocatalytic activities for ORR.[16] In contrast, Li et al. have demonstrated that nitrogen-functionalized GQDs had highly size-dependent electrocatalytic activity.[17] More recently, mixing C quantum dots with heteroatom-doped C nanotubes[18] or graphene[19] has also been demonstrated to show synergistic effects to enhance the ORR electrocatalytic activity.

The much improved catalytic performance of heteroatom-doped C materials has been attributed to the doping-induced charge/spin redistributions, which changed the chemisorption mode of O_2 and/or reduced the ORR potential to facilitate ORR at the doped C electrode.[5a,20] In contrast, a 4e ORR electrocatalytic activity has rarely been reported for undoped C nanomaterials.[21] In this study, we developed a new class of undoped ORR catalysts based on GQDs supported by graphene nanoribbons (GNRs) through a one-step simultaneous reduction reaction, leading to ultrahigh performance for O reduction via a 4e ORR process with excellent electrocatalytic activity (ultrahigh limiting current density and low overpotential) and high selectivity and stability in alkaline media comparable to the best C-based ORR catalysts reported so far.[4−19] The GQD-GNR hybrids were prepared through a template-free simultaneous reduction reaction of two reactants (i.e., methylbenzene and hexabromobenzene) by Na via Scheme 1.

Scheme 1. Formation of GQD-GNR Hybrid

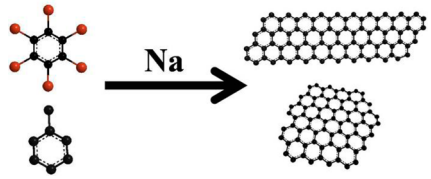

As far as we are aware, this is the first solution reaction for the formation of GNRs from low molecular weight (LMW) reactants, whereas hydrothermal reactions to C dots from LMW precursors have been recently reported.[22] Figure 1 shows typical TEM images of the newly synthesized materials under different magnifications. At a low magnification (Figure 1a,b), the resulting materials appear as a treelike fractal structure with numerous nanoribbon branches. An enlarged view in Figure 1c shows many dots dispersed on the surface of those nanoribbons. Careful examination of the dots under even higher magnification

Received: April 13, 2015
Published: June 8, 2015

DOI: 10.1021/jacs.5b03799
J. Am. Chem. Soc. 2015, 137, 7588−7591

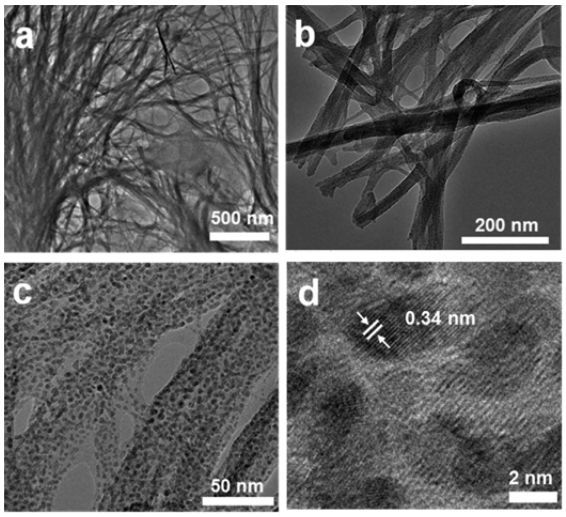

Figure 1. T(a–c) EM and (d) HRTEM images of the as-prepared hierarchically structured GQD-GNR hybrid.

reveals that they are GQDs with an average size of about 5 nm and lattice spacing of 0.34 nm, corresponding to the (002) facet of graphitic C (Figure 1d).

In a typical experiment, a large chunk (~0.6 g) of Na with a shining surface, 30 mL of methylbenzene, and 0.3 g of hexabromobenzene were added to a 50 mL stainless-steel reactor (Parr Instrument Company, America, model 5500). The sealed reactor was then placed in an oil bath to react under constant stirring for 20 h at 220 °C, followed by annealing the product under Ar at 1000 °C for 2 h. It was found that annealing at 1000 °C resulted in the largest specific surface area (158 m^2/g) and pore volume (0.29 cm^3/g) among all the samples studied in this work (Table S1). Our control experiments demonstrated that the reaction between methylbenzene and Na alone produced GNRs (Figure S1), whereas quantum dots were the dominant product from the reaction of hexabromobenzene with Na (Figure S2). As illustrated in Scheme 1, it is the simultaneous reduction of methylbenzene and hexabromobenzene by Na that is responsible for the formation of the GQD-GNR hybrid. The intimate contact between the GQDs and GNRs seen in Figure 1c,d could effectively prevent GQDs from aggregation and, more importantly, ensure efficient charge-transfers between them; both are advantages for ORR electrocatalysis.

The Fourier transform infrared (FTIR) spectrum of the GQD-GNR hybrid is given in Figure 2a; two peaks at 1580 and 1436 cm^{-1} are most probably due to the presence of conjugated and isolated C=C bonds in the graphitic structure where defects are evident. In addition, a broad band over 1000–1300 cm^{-1}, attributable to the aromatic C–H in-plane bending vibration, was also found. Figure 2b reproduces an XPS survey spectrum for the GQD-GNR supported by a SiO_2-coated Si wafer, which shows only C 1s and very weak but noticeable O 1s peaks. The high-resolution C 1s spectrum shown in the inset of Figure 2b is very similar to that of graphite (HOPG),[23] suggesting that the GQD-GNR structure is free from C-bonded O. This, together with the absence of Si signal in Figure 2b, indicates that the O 1s peak most probably arises from physically adsorbed O because graphitic C is known to be susceptible to O adsorption even at pressures as low as 10^{-8}–10^{-10} Torr,[24] typical for the XPS measurements (Figure S4). The strong O adsorption capacity (0.2 w/w%; Supporting Information) offers an additional advantage for ORR electrocatalysis. The absence of Na signal

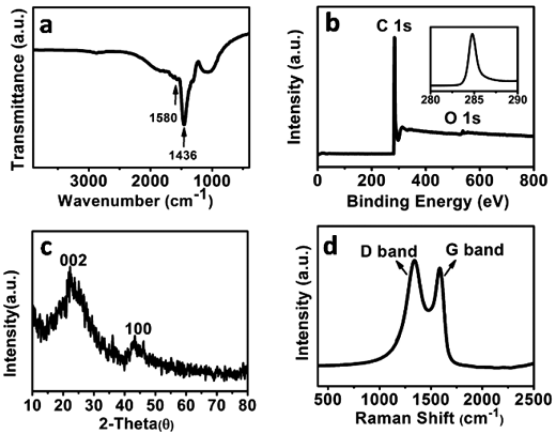

Figure 2. Structural and compositional characterization for the GQD-GNR hybrid: (a) FTIR, (b) XPS, (c) XRD, and (d) Raman.

from Figure 2b indicates that Na residue, if any, has been completely removed during the postsynthesis workup process. The ICP-MS measurements (Supporting Information) indicate that the GQD-GNR hybrids contain about 18.0 ppm Fe, 0.5 ppm of Co, and 0.8 ppm Mn, which most likely come from impurity of the starting materials. The XRD pattern given in Figure 2c shows two peaks corresponding to (100) and (002) facets, respectively, of graphitic C. Though both are somewhat broad, the relatively high peak intensity of the D band with respect to that of the G band seen in the Raman spectrum given in Figure 2d indicates the presence of a large number of edges/defects in the GQD-GNR hybrid, which is another advantage for electrocatalysis of ORR because defects and edges are known to provide active sites in electrocatalytic reactions.[25]

Electrocatalytic performance of the GQD-GNR hybrid was investigated with cyclic voltammetry (CV) in a N_2- and O_2-saturated 0.1 M KOH solution at a scan rate of 10 mV s^{-1}. Figure 3a shows a single cathodic reduction peak at −0.19 V (vs. Ag|AgCl electrode) in the O_2-saturated KOH solution; in contrast, only capacitive behavior was seen in the N_2-saturated solution. As expected, these results clearly indicate that the GQD-GNR hybrid has a pronounced catalytic activity for ORR. To further

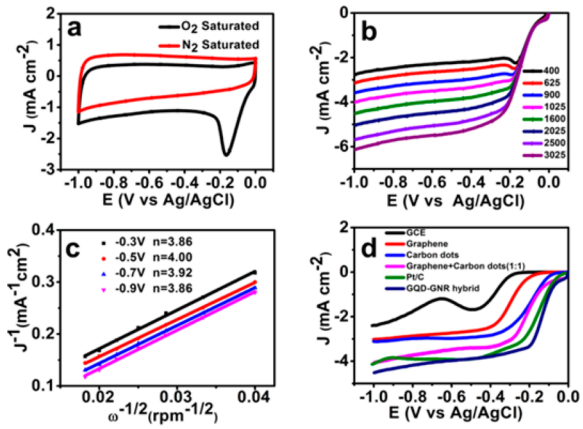

Figure 3. (a) CVs in O_2-saturated (black) and N_2-saturated (red) 0.1 M KOH. (b) LSV of O-saturated solution under different rotating rates of the disc electrode. (c) Koutecky–Levich plots (J^{-1} versus $\omega^{-1/2}$) at different electrode potentials. (d) LSV of O_2-saturated 0.1 KOH solution at working electrodes prepared with different electrocatalysts at a disk rotating rate of 1600 rpm and a scanning rate of 10 mV s^{-1}.

DOI: 10.1021/jacs.5b03799
J. Am. Chem. Soc. 2015, 137, 7588–7591

evaluate kinetics of the ORR at the GQD-GNR electrode, linear sweep voltammetry (LSV) was recorded in an O_2-saturated 0.1 M KOH electrolyte using a rotating disk electrode (RDE) at a scan rate of 10 mV s^{-1}. Figure 3b shows ORR polarization curves at different rotating rates. As expected, the catalytic current density increased with increasing the electrode rotating rate.

The corresponding Koutecky–Levich (K–L) plots at −0.3, −0.5, −0.7, and −0.9 V are shown in Figure 3c, from which the transferred electron number (n) per O molecule at the GQD-GNR electrode was calculated via the K–L equation[26] to be about 3.91, characteristic of a one-step 4e ORR process. We also employed a rotating-ring disk electrode (RRDE) to measure the amount of H_2O_2 produced in the above process (Figure S6). The measured H_2O_2 yield is below ∼5.5%, over the potential range of −0.9 to −0.3 V, giving an electron transfer number of ∼3.90. This is consistent with the result obtained from the K–L plots (Figure 3c) that are based on the RDE measurements, confirming that ORR catalyzed by the GQD-GNR hybrid is mainly through a 4e pathway (Supporting Information). Because the catalyst loading was reduced from 0.6 to 0.1 mg cm^{-2}, the H_2O_2 production increased slightly to 7% (Supporting Information), indicating a negligible effect of the catalyst thickness on the H_2O_2 generation.[28] The Tafel slope measured with the GQD-GNR hybrid catalyst is ∼87.7 mV per decade, which is similar to that of the Pt/C catalyst (Supporting Information). We also evaluated the electrocatalytic performance of the above GQD-GNR electrode against commercial Pt/C catalysts (40%, Vulcan XC-72R), commercial graphene, and C quantum dots of a similar impurity population as that of their counterparts synthesized in this study (XFNANO Materials Tech Co., Ltd., China), and a mixture of the commercial C quantum dots and graphene. (See Supporting Information for detailed characterization.) Figure 3d shows LSVs recorded in the O_2-saturated solution for the graphene, C dots, graphene/C dot mixture, GQD-GNR hybrid, and Pt/C (40%) electrodes, along with a glassy-carbon electrode (GCE), at a rotating rate of 1600 rpm and scanning rate of 10 mV s^{-1}. It is important to note that the onset potential of ORR at the GQD-GNR electrode is even more positive than that of Pt/C (Figure S14), indicating excellent ORR performance for this newly developed electrocatalyst. As far as we are aware, this is one of a few C-based ORR catalysts with a more positive onset potential than that of Pt/C.[10e,14c] The half-wave potential of the GQD-GNR electrode is as good as that of the Pt/C catalyst but much better than that of the GQD (C dots) and graphene alone (Figure 3d). The fact that our GQD-GNR hybrid greatly outperformed the mixture of commercial graphene and GQD (Figure 3d) highlights the importance of the intimate contact between GQD and GNR components for an efficient charge transfer to the ORR performance. As seen in Figure S9, the Raman (G) band of the GQD-GNR hybrid shows a slight but noticeable upshift with respect to those of the GQD and a downshift to those of GNR, presumably because of charge transfer from the GQD to GNR.[11a,27]

Stability of the GQD-GNR electrode was also tested under a constant potential of −0.4 V in O_2-sturated 0.1 M KOH at an electrode rotation rate of 800 rpm. As seen in Figure 4a, the GQD-GNR electrode exhibited an excellent durability with only about 1% decrease in current after 26 h. For comparison, the activity of 40% Pt/C catalysts was also tested under the same conditions and showed a much more pronounced decrease (∼70%, Figure 4a). The observed high current retention for the GQD-GNR electrode is also much better than those reported for most other heteroatom-doped graphene catalysts.[12] Figure 4b

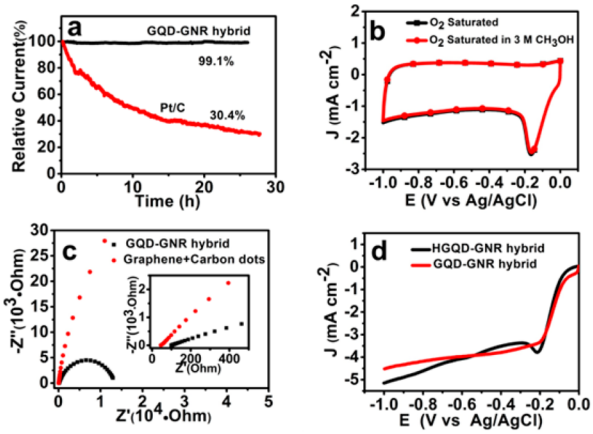

Figure 4. (a) Durability test of the GQD-GNR electrode in O_2-saturated 0.1 M KOH. (b) CV of the GQD-GNR electrode in an alkaline solution (0.1 M KOH) with or without methanol. (c) EIS of electrodes prepared with GQD-GNR or mixture of graphene and C dots. (d) LSV of O_2-saturated 0.1 KOH solution at working electrodes prepared with GQD-GNR or HGQD-GNR electrocatalysts at a disk rotating rate of 1600 rpm and a scanning rate of 10 mV s^{-1}.

shows CV of the GQD-GNR electrode in O_2-saturated 0.1 M KOH solution before and after adding CH_3OH (3 M). The almost identical CV spectra shown in Figure 4b indicate a good tolerance of the GQD-GNR electrode to CH_3OH crossover effect encountered frequently in fuel cells. Clearly, the GQD-GNR hybrid is a very promising C-based catalyst in direct fuel cells operated in alkaline. Figure 4c shows electrochemical impedance spectra at the electrodes prepared with the GQD-GNR hybrid with respect to a mixture of commercial graphene and C dots. The significantly low resistance of the GQD-GNR hybrid indicates that the intimate interaction between the GNR and GQD is crucial for the observed electrocatalytic activity. This is because the ORR activity of the GQD-GNR hybrid is originated from the charge transfer between the GQD and GNR, as is the case for the doping-induced charge-transfer in heteroatom-doped C catalysts.[11,20b] To ensure that Na did not contribute to the observed outstanding performance of the GQD-GNR electrode, the as-prepared GQD-GNR electrode was subjected to H treatment (HGQD-GNR) to further remove Na residue, if any. As seen in Figure 4d, the GQD-GNR and HGQD-GNR electrodes exhibited almost the same electrocatalytic activity without any obvious Na effect. CN^- was also introduced in our experiments to poison other metal residues;[29] the LSVs, once again, show no difference (Supporting Information). Thus, the observed ORR catalytic activity for the GQD-GNR electrode can be exclusively attributed to the C active sites caused by charge transfer between the intimately contacted GQD and GNR (vide supra).

We synthesized hierarchically structured GNRs with uniformly interdispersed GQDs simply through one-step coreduction of methylbenzene and bromobenzene by Na. The resultant GQD-GNR hybrid exhibited a more positive onset potential and higher diffusion current density for ORR than those of the commercial Pt/C (40%) catalyst with a much better durability and tolerance to methanol crossover effect that were comparable to the best metal-free and other ORR catalysts reported so far. The superb ORR performance observed for the undoped all-C GQD-GNR hybrid was attributed to the charge transfer between the intimately contacted GQD and GNR components, along with the numerous surface/edge defects on the GQD/GNR

DOI: 10.1021/jacs.5b03799
J. Am. Chem. Soc. 2015, 137, 7588–7591

surfaces and at their interface to act as the active sites. This study offers a new direction for large-scale development of low-cost, C-based ORR electrocatalysts with superb ORR performance.

■ ASSOCIATED CONTENT

Supporting Information

Detailed experimental procedures and characterization data. The Supporting Information is available free of charge on the ACS Publications website at DOI: 10.1021/jacs.5b03799.

■ AUTHOR INFORMATION

Corresponding Authors

*shunwang@wzu.edu.cn
*lxd115@case.edu
*jwang@uwindsor.ca

Notes

The authors declare no competing financial interest.

■ ACKNOWLEDGMENTS

We are grateful for financial support from NSFC (51272182, 21471116, and 21301130), Zhejiang Provincial Natural Science Foundation of China (LY13E020008 and Z15E020005) and NSF (CMMI-1266295, CMMI-1400274, and AIR-IIP-1343270).

■ REFERENCES

(1) (a) Debe, M. K. *Nature* **2012**, *486*, 43. (b) Cheng, F. Y.; Chen, J. *Chem. Soc. Rev.* **2012**, *41*, 2172. (c) Dai, L.; Xue, Y.; Qu, L.; Choi, H.-J.; Baek, J.-B. *Chem. Rev.* **2015**, DOI: 10.1021/cr5003563.

(2) (a) Cheng, A. C.; Holt-Hindle, P. *Chem. Rev.* **2010**, *110*, 3767. (b) Bing, Y. H.; Liu, H. S.; Zhang, L.; Ghosh, D.; Zhang, J. J. *Chem. Soc. Rev.* **2010**, *39*, 2184. (c) Wu, J. B.; Yang, H. *Acc. Chem. Res.* **2013**, *46*, 1848. (d) Liu, Y.; Mustain, W. E. *J. Am. Chem. Soc.* **2013**, *135*, 530.

(3) (a) Gasteiger, H. A.; Markovic, N. M. *Science* **2009**, *324*, 48. (b) Morozan, A.; Jousselme, B.; Palacin, S. *Energy Environ. Sci.* **2011**, *4*, 1238.

(4) (a) Wu, G.; More, K. L.; Johnston, C. M.; Zelenay, P. *Science* **2011**, *332*, 443. (b) Wu, G.; Zelenay, P. *Acc. Chem. Res.* **2013**, *46*, 1878. (c) Liang, H. W.; Wei, W.; Wu, Z. S.; Feng, X. L.; Müllen, K. *J. Am. Chem. Soc.* **2013**, *135*, 16002.

(5) (a) Gong, K.; Du, F.; Xia, Z.; Durstock, M.; Dai, L. *Science* **2009**, *323*, 760. (b) Winther-Jensen, B.; Winther-Jensen, O.; Forsyth, M.; MacFarlane, D. R. *Science* **2008**, *321*, 671. (c) Zhao, Y.; Watanabe, Kazuya; Hashimoto, K. *J. Am. Chem. Soc.* **2012**, *134*, 19528. (d) Jiao, Y.; Zheng, Y.; Jaroniec, M.; Qiao, S. Z. *J. Am. Chem. Soc.* **2014**, *136*, 4394. (e) Yang, S. B.; Feng, X. L.; Wang, X. C. *Angew. Chem., Int. Ed.* **2011**, *50*, 5339. (f) Yu, D.; Nagelli, E.; Dai, L. *J. Phys. Chem. Lett.* **2010**, *1*, 2165.

(6) (a) Carver, C. T.; Matson, B. D.; Mayer, J. M. *J. Am. Chem. Soc.* **2012**, *134*, 5444. (b) Wang, Q.; Zhou, Z. Y.; Lai, Y. J.; You, Y.; Liu, J. G.; Wu, X. L.; Terefe, E.; Chen, C.; Song, L.; Rauf, M.; Tian, N.; Sun, S. G. *J. Am. Chem. Soc.* **2014**, *136*, 10882.

(7) (a) Gao, M. R.; Xu, Y. F.; Jiang, J.; Yu, S. H. *Chem. Soc. Rev.* **2013**, *42*, 2986. (b) Faber, M. S.; Lukowski, M.; Ding, Q.; Kaiser, N. S.; Jin, S. *J. Phys. Chem. C* **2014**, *118*, 21347.

(8) (a) Liang, Y. Y.; Wang, H. L.; Zhou, J. G.; Li, Y. G.; Wang, J.; Regier, T.; Dai, H. J. *J. Am. Chem. Soc.* **2012**, *134*, 3517. (b) Wu, Z. S.; Yang, S. B.; Sun, Y.; Parvez, K.; Feng, X. L.; Müllen, K. *J. Am. Chem. Soc.* **2012**, *134*, 9082.

(9) (a) Lin, L.; Zhu, Q.; Xu, A. W. *J. Am. Chem. Soc.* **2014**, *136*, 11027. (b) Gao, M. R.; Xu, Y. F.; Jiang, J.; Yu, S. H. *Chem. Soc. Rev.* **2013**, *42*, 2986.

(10) (a) Su, D. S.; Perathoner, S.; Centi, G. *Chem. Rev.* **2013**, *113*, 5782. (b) Zheng, Y.; Jiao, Y.; Ge, L.; Jaroniec, M.; Qiao, S. Z. *Angew. Chem., Int. Ed.* **2013**, *52*, 3110. (c) Jeon, I. Y.; Zhang, S.; Zhang, L.; Choi, H. J.; Seo, J. M.; Xia, Z.; Dai, L.; Baek, J. B. *Adv. Mater.* **2013**, *25*, 6138. (d) Zhang, C. Z.; Mahmood, N.; Yin, H.; Liu, F.; Hou, Y. L. *Adv. Mater.* **2013**, *25*, 4932. (e) Sun, X. J.; Song, P.; Zhang, Y. W.; Liu, C. P.; Xu, W. L.; Xing, W. *Sci. Rep.* **2013**, *3*, 2505. (f) Dai, L.; Chang, D.; Baek, J.-B.; Lu, W. *Small* **2012**, *8*, 1130.

(11) (a) Wang, S.; Iyyamperumal, E.; Roy, A.; Xue, Y.; Yu, D.; Dai, L. *Angew. Chem., Int. Ed.* **2011**, *50*, 11756. (b) Hijazi, I.; Bourgeteau, T.; Cornut, R.; Morozan, A.; Filoramo, A.; Leroy, J.; Derycke, V.; Jousselme, B.; Campidelli, S. *J. Am. Chem. Soc.* **2014**, *136*, 6348. (c) Zhao, Y.; Yang, L. J.; Chen, S.; Wang, X. Z.; Ma, Y. W.; Wu, Q.; Jiang, Y. F.; Qian, W. J.; Hu, Z. *J. Am. Chem. Soc.* **2013**, *135*, 1201.

(12) (a) Zhang, C. Z.; Mahmood, N.; Yin, H.; Liu, F.; Hou, Y. L. *Adv. Mater.* **2013**, *25*, 4932. (b) Wang, X. W.; Sun, G. Z.; Routh, P.; Kim, D. H.; Huang, W.; Chen, P. *Chem. Soc. Rev.* **2014**, *43*, 7067. (c) Jeon, I. Y.; Choi, H. J.; Jung, S. M.; Seo, J. M.; Kim, M. J.; Dai, L.; Baek, J. B. *J. Am. Chem. Soc.* **2013**, *135*, 1386. (d) Yang, Z.; Yao, Z.; Li, G. F.; Fang, G. Y.; Nie, H. G.; Liu, Z.; Zhou, X. M.; Chen, X. A.; Huang, S. M. *ACS Nano* **2012**, *6*, 205.

(13) (a) Chen, S.; Bi, J.; Zhao, Y.; Yang, L.; Zhang, C.; Ma, Y.; Wu, Q.; Wang, X.; Hu, Z. *Adv. Mater.* **2012**, *24*, 5593. (b) Zheng, Y.; Jiao, Y.; Chen, J.; Liu, J.; Liang, J.; Du, A. J.; Zhang, W. M.; Zhu, Z. H.; Smith, S. C.; Jaroniec, M.; Lu, G. Q.; Qiao, S. Z. *J. Am. Chem. Soc.* **2011**, *133*, 20116.

(14) (a) Wang, J.; Jin, H. L.; He, Y. H.; Lin, D. J.; Liu, A. L.; Wang, S.; Wang, J. C. *Nanoscale* **2014**, *6*, 7204. (b) Aijaz, A.; Fujiwara, N.; Xu, Q. *J. Am. Chem. Soc.* **2014**, *136*, 6790. (c) Yang, W.; Fellinger, T. P.; Antonietti, M. *J. Am. Chem. Soc.* **2011**, *133*, 206.

(15) (a) Liang, J.; Jiao, Y.; Jaroniec, M.; Qiao, S. Z. *Angew. Chem., Int. Ed.* **2012**, *51*, 11496. (b) Lin, Z. Y.; Waller, G.; Liu, Y.; Liu, M. L.; Wong, C. P. *Angew. Chem., Int. Ed.* **2012**, *2*, 884. (c) Silva, R.; Voiry, D.; Chhowalla, M.; Asefa, T. *J. Am. Chem. Soc.* **2013**, *135*, 7823. (d) Zhang, M.; Dai, L. *Nano Energy* **2012**, *4*, 514.

(16) Li, Y.; Zhao, Y.; Cheng, H. H.; Hu, Y.; Shi, G. Q.; Dai, L. M.; Qu, L. T. *J. Am. Chem. Soc.* **2012**, *134*, 15.

(17) Li, Q.; Zhang, S.; Dai, L.; Li, L. *J. Am. Chem. Soc.* **2012**, *134*, 18932.

(18) Zhou, X. M.; Tian, Z. M.; Li, J.; Ruan, H.; Ma, Y. Y.; Yang, Z.; Qu, Y. Q. *Nanoscale* **2014**, *6*, 2603.

(19) Fei, H. L.; Ye, R. Q.; Ye, G. L.; Gong, Y. J.; Peng, Z. W.; Fan, X. J.; Samuel, E. L. G.; Ajayan, P. M.; Tour, J. M. *ACS Nano* **2014**, *8*, 10837.

(20) (a) Cheon, J. Y.; Kim, J. H.; Kim, J. H.; Goddeti, K. C.; Park, J. Y.; Joo, S. H. *J. Am. Chem. Soc.* **2014**, *136*, 8875. (b) Dai, L. *Acc. Chem. Res.* **2013**, *46*, 31. (c) Qu, L. T.; Dai, L. M.; Stone, M.; Xia, Z. H.; Wang, Z. L. *Science* **2008**, *322*, 238.

(21) Wei, W.; Tao, Y.; Lv, W.; Su, F. Y.; Ke, L.; Li, J.; Wang, D. W.; Li, B. H.; Kang, F. Y.; Yang, Q. H. *Sci. Rep.* **2014**, *4*, 6289.

(22) See, for example, (a) Wickramaratne, N.; Xu, J.; Wang, M.; Zhu, L.; Dai, L.; Jaroniec, M. *Chem. Mater.* **2014**, *26*, 2820. (b) Jiang, L.; Niu, T. C.; Lu, X. Q.; Dong, H. L.; Chen, W.; Liu, Y. Q.; Hu, W. P.; Zhu, D. B. *J. Am. Chem. Soc.* **2013**, *135*, 9050.

(23) Yudasaka, M.; Kikuchi, R.; Ohki, Y.; Yoshimura, S. *Carbon* **1997**, *35*, 195.

(24) Collins, P. G.; Bradley, K.; Ishigami, M.; Zettl, A. *Science* **2000**, *287*, 1801.

(25) (a) Yuan, W. J.; Zhou, Y.; Li, Y. R.; Li, C.; Peng, H. L.; Zhang, J.; Liu, Z. F.; Dai, L. M.; Shi, G. Q. *Sci. Rep.* **2013**, *3*, 2248. (b) Deng, D. H.; Yu, L.; Pan, X. L.; Wang, S.; Chen, X. Q.; Hu, P.; Sun, L. X.; Bao, X. H. *Chem. Commun.* **2011**, *47*, 10016. (c) Chung, H. T.; Won, J. H.; Zelenay, P. *Nat. Commun.* **2013**, *4*, 1922. (d) Shen, A.; Zou, Y.; Wang, Q.; Dryfe, R.; Huang, X.; Dou, S.; Dai, L.; Wang, S. *Angew. Chem., Int. Ed.* **2014**, *53*, 10804.

(26) Yu, D. S.; Zhang, Q.; Dai, L. M. *J. Am. Chem. Soc.* **2010**, *132*, 15127.

(27) Shin, H.-J.; Kim, S. M.; Yoon, S.-M.; Benayad, A.; Kim, K. K.; Kim, S. J.; Park, H. K.; Choi, J.-Y.; Lee, Y. H. *J. Am. Chem. Soc.* **2008**, *130*, 2062.

(28) Bonakdarpour, A.; Lefevre, M.; Yang, R. Z.; Jaouen, F.; Dahn, T.; Dodelet, J. P.; Dahn, J. R. *Electrochem. Solid-State Lett.* **2008**, *11*, B105.

(29) Li, Y. G.; Zhou, W.; Wang, H. L.; Xie, L. M.; Liang, Y. Y.; Wei, F.; Idrobo, J. C.; Pennycook, S. J.; Dai, H. J. *Nat. Nanotechnol.* **2012**, *7*, 394.

DOI: 10.1021/jacs.5b03799
J. Am. Chem. Soc. 2015, 137, 7588−7591